Mirror contamination and secondary electron effects during EUV reflectivity analysis

M. Catalfano[a], A. Kanjilal[a], A. Al-Ajlony[a], S. S. Harilal[a], A. Hassanein[a], and B. Rice[b]

[a]Center for Materials Under Extreme Environment, School of Nuclear Engineering,
Purdue University, West Lafayette, IN 47907, USA;
[b]SEMATECH Inc., Albany, NY 12203, USA

ABSTRACT

We investigated Ru mirror contamination and subsequent EUV reflectivity loss using the IMPACT facility at Purdue University. Because Ru can either be used as a grazing mirror or as a capping layer for multilayer normal mirror, we examined the angular dependency of XPS peak area intensity at the O 1*s* and Ru 3*d* regions as well as the effects of sputtering. Although no change in intensity has been observed at lower take-off angles from the target surface, the peak area intensity starts changing with increasing θ (i.e., emission observation angle, representing the angle between the target surface plane and detector entrance). Among different components, the effect of water and oxidized carbon are found to be most notable when viewed at lower θ, and primarily responsible for degrading the reflectivity of the Ru layer. On the other hand, the effect of OH becomes dominant with increasing observation angle θ, and thus plays a key role to suppress optical transmission. Moreover, atomic carbon effect is found to peak when observed at 30^o, and most likely plays an important role in degrading both reflectivity and transmission. This is also because of the total photon path length in the Ru film at different angles. During the contamination process, the EUV reflectivity of the Ru film is found to significantly degrade in the presence of additional secondary electrons from the focusing Ru mirror of the EUV setup. This effect could be explained in the light of a competition between oxidation and carbonization processes on Ru surface.

Keywords: Extreme ultraviolet lithography, Mirror contamination, Ru mirror, EUV Reflectivity, Secondary electrons, X-ray photoelectron spectroscopy

1. INTRODUCTION

Next generation computer chips require features as small as 20 nm. To meet this goal, future photolithography systems are looking to employ extreme ultraviolet (EUV) radiation at the wavelength of 13.5 nm. The mirrors to be used in these systems consist of alternating layers of Mo and Si[1]. Because there are concerns about potential oxidation of the surface Si layer, a thin Ru protective layer has often been used on the top Si layer[1]. A Mo/Si multilayer mirror with a Ru capping layer can reflect up to 70 % of the EUV light[2] near normal incidence[3]. Ru films can also reflect 92 eV photons at a grazing angle[4]. Since short wavelengths can be attenuated by most materials,[5] an EUV lithography system, therefore, requires a vacuum chamber. Now the question is how to keep the Ru optics free of carbon and oxygen, as contaminants are often formed during EUV exposure. Several cleaning processes[1] have been proposed to mitigate this problem. It has been shown that the secondary electrons (SEs) from the Ru surface take part in dissociating water and/or hydrocarbons under EUV radiation,[6] creating chemically active fragments on the Ru surface[7].

Since several mirrors will be used in an EUV lithography (EUVL) setup,[5] a 1% loss of mirror reflectivity would degrade the mirror performance beyond the expected lifetime[8]. Although recent studies have been done on electron-assisted deposition of carbon on the Ru surface[8] to simulate the surface chemistry during EUV radiation, the effect of additional SEs from successive mirrors on the reflectivity has not yet been evaluated. In fact, SEs can be expected to reach from mirror to mirror along with the EUV photons. Although several reports are available in the literature that deal with EUV radiation induced growth of contaminants on Ru surfaces,[9] knowledge of interaction of EUV photons with various adsorbed species is still scarce. It is also important to evaluate what role SEs play on the reflectivity of the system. In this article, using X-Ray photoelectron spectroscopy, we examine the angular properties of typical contaminants that can

Extreme Ultraviolet (EUV) Lithography III, edited by Patrick P. Naulleau,
Obert R. Wood II, Proc. of SPIE Vol. 8322, 832233 · © 2012 SPIE
CCC code: 0277-786X/12/$18 · doi: 10.1117/12.916417

form on Ru in vacuum chamber. We also studied the differences that occur in the contaminant formation with and without SEs from the ruthenium surface. Finally, we studied the reflectivity in the presence of SEs.

2. EXPERIMENTAL SETUP

The experiments were performed at the IMPACT materials characterization laboratory in CMUXE which contains an UHV chamber equipped with a suite of *in situ* diagnostic tools for surface analysis including XPS, extreme ultraviolet photoelectron spectroscopy (EUPS), AES, low-energy ion scattering spectroscopy, and extreme ultraviolet reflectivity (EUVR). To create a chamber conditions similar to that of the EUVL system,[10] we did not bake our UHV chamber giving a base pressure of ~1.4×10^{-8} Torr. The XPS measurements at different stages of our experiments were performed using an Al-K_α radiation source ($h\nu$ = 1486.65 eV) where the photoelectrons (PEs) from the target surface were analyzed with a SPECS Phoibos-100 hemispherical electron analyzer (resolution of 0.85 eV). The data were recorded for θ (i.e., emission observation angle, representing the angle between the surface normal and the z coordinate direction.) in the range of 0^o to 50^o with φ kept at 45^o (see Fig. 1). Calibration of binding energy (BE) scale with respect to the measured kinetic energy (KE) was made using the silver Fermi energy edge. Grazing incidence EUVR of Ru films has been investigated with the help of a Phoenix EUV source[11] that emits light in the range of 12.5-15 nm with a peak maximum at ~13.5 nm (92 eV), and two calibrated EUV photodiodes (PDs) from International Radiation Detectors Inc.

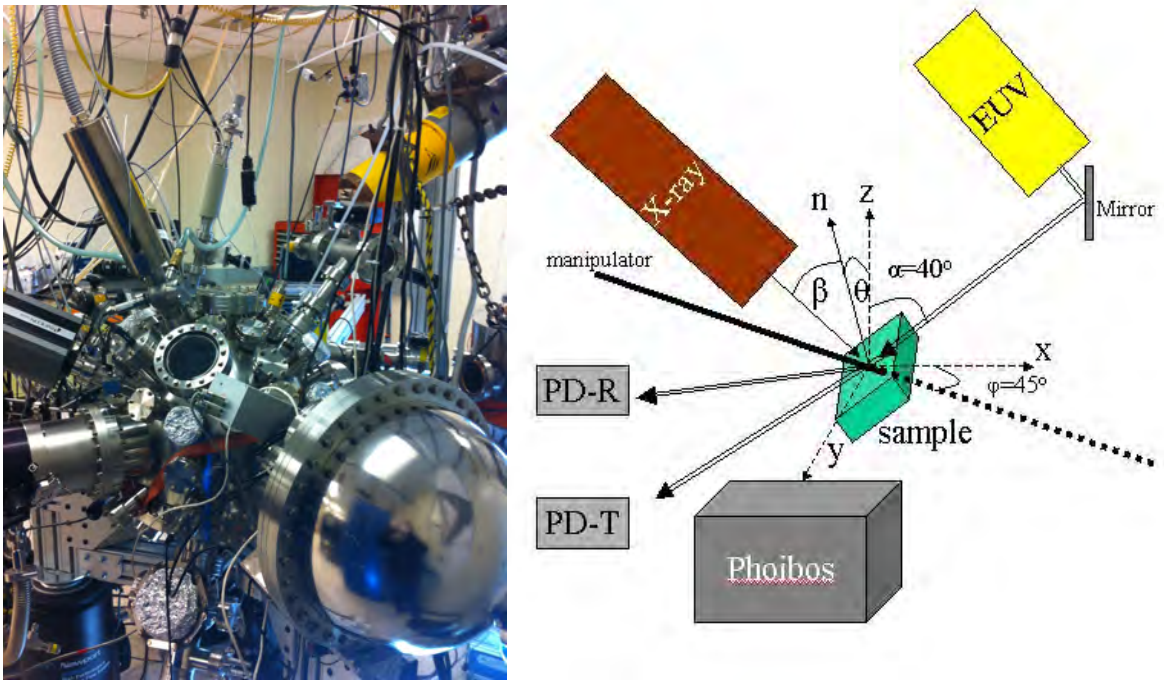

Figure 1: Left: photograph of IMPACT facility at Purdue University. Right: Schematic of chamber. The sample manipulator is kept at φ=45^o from the x-axis of a coordinate system. The emission angle, representing the angle between the target surface normal and the z coordinate direction is designated as. θ. The angle between the x-ray source and the sample normal is designated as β. The EUV beam is situated at α=40^o from the z-axis. The photoelectrons produced in the experiment enter Phoibos, the hemispherical electrostatic energy analyzer. Two photodiodes (PD-T and PD-R) help to measure the EUV reflectivity of the sample.

The target holder is insulated from the chamber and the sample current was measured from the target in series with a grounded Keithley-6487 pico-ammeter. The 92 eV photons from the compact EUV source are projected onto the Ru surface with the help of an ellipsoidal Ru mirror situated 21 inches away from the target surface. Since this mirror is also used to remove stray X-rays and the Bremsstrahlung radiation from the EUV source,[12] it is capable to produce PEs. As in the present EUV setup it is impossible to clean the Ru mirror frequently, contaminating molecules on the Ru surface lead to the emission of SEs[13]. However, the mirror itself is not subject to bombardment by electrons. To screen out these energetic SEs, a magnet has been employed to deflect the additional electrons from the EUV ray path, showing a drastic

change in the sample current from -1.1 nA to 0.5 nA. The EUVR has been recorded both in the presence and absence of these additional electrons from the focusing Ru mirror.

A 50 nm Ru film grown on a *p*-type Si(100) wafer was diced into several pieces with an average area of 1×1 cm^2. The Ru surface was sputter cleaned with 2 keV Ar^+ giving a sample current of ~800 nA. Each sample was examined *in situ* by means of XPS to assess the contamination level. Prior to examining the EUVR, the beam was adjusted using a through-PD in such a way that the focused beam on the Ru surface provides maximum intensity in the reflected-PD with the spot size as big as the area of the investigating samples. The Ru sample was examined by changing the emission angle, both with sputtering and without. Then, reflectivity analysis was taken before and after sputtering, as well as after EUV both with and without SEs.

3. RESULTS AND DISCUSSION

Typical observed emission angle dependent XPS results are shown in Fig. 2. As can be seen, strong water and carbon peaks are immediately visible in O 1*s* and Ru 3*d* regions, respectively. Since the reflection and transmission properties of a Ru layer depend on incidence angle of the 13.5 nm EUV light, this study may shed light on how the adsorbents on Ru surface are oriented/distributed and the anisotropic behavior of adsorbed molecules. Normally, by neglecting the angle dependent change in ionization cross-section of a core level of an atom and elastic scattering of electrons, angle-resolved XPS (ARXPS) is commonly used for depth profiling of atoms. This process is only suitable if a homogeneous layer is formed on surface[14]. However, because the photoionization cross-section depends strongly on incident angle[15], it can also be used to examine the orientation of adsorbed molecules on the surface. The polarization direction of the incident radiation affects electron transition of dipole matrix element, which is governed by the parity of the final state wave function, the operator **A.P** (dot product of ionization vector and momentum vector), and the initial state wave function (see Ref. 14 for details). According to the geometry of our chamber, when the incidence angle β is 25°, then θ = 0°. Therefore, when θ increases from 0° to 50°, β changes from 25° to – 25° (see Fig. 1). Hence, the interaction between the beam and the molecular components will vary with increasing β if they have chemical anisotropy. This experiment examined two kinds of Ru conditions, as shown in Fig. 2. The first was only sputtered once at the beginning of the experiment (solid lines) while the second was sputter cleaned between each exposure (dotted lines). This shows the effect of the buildup of adsorbents on the Ru surface with θ.

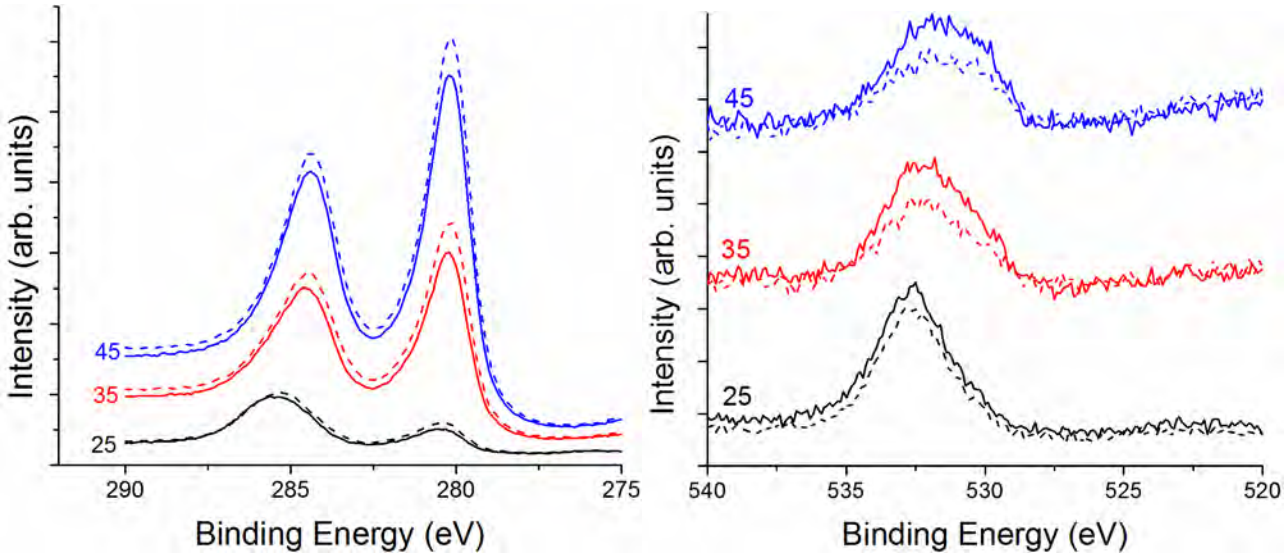

Figure 2: XPS spectra of Ru 3*d* region (left) and O1*s* region (right) of the ruthenium film. Spectra sputtered between each exposure appear in dashed lines, while solid lines represent the sample which was sputtered once in the beginning of the XPS data acquisition.

In Figure 2, it appears that the change in intensity is pronounced at higher observed θ. This is because of the C-O_n and water molecules, which are bound directly to the Ru surface in the first layer (will be discussed in the following), and dominate at lower θ due to their orientations with regard to the incident beam. However, there is a clear difference in

intensity between the sample which was sputtered between each region and the one time sputtered sample. We believe that more and more contaminants are coming on Ru with time in the once sputtered case, and thereby contributing to the overall photoemission yield by suppressing the Ru signal. Meanwhile, the XPS signal at the Ru 3*d* region becomes weak due to poor photoionization of carbon in the presence of a limited number of molecules in an anisotropic environment of adsorbed layers. Thus, the Ru 3*d* spin-orbit doublet peaking around 280.1 and 284.9 eV, respectively, becomes prominent for $\theta > 35^{o}$.

For in-depth understanding of the phenomena, XPS spectra recorded at various θ have been deconvoluted into components using conventional fitting procedure, the results of which are shown in Fig. 3. The components used are the chemically active fragments that typically result from the dissociation of hydrocarbons and/or water molecules by SEs[6]. We have considered here only the components associated with the adsorbents on the Ru surface. In particular, we found that H_2O (532.6 eV) and OH (530.75 eV)[16] are the components of interest at the O 1*s* region, while the Ru 3*d* region consists of carbon (284.6 eV) and oxidized carbon (*i.e.*, C-O_n), which includes both O-C=O (288.6 eV) and C-O (286.4 eV) bonds[17]. The relative change in peak (area) intensity of water molecules and OH, and the carbon and C-O_n are plotted in Fig. 3. Although β was kept near normal to the Ru surface (25^{o} to -25^{o}), there still exists a large change in polarization of the molecular components. This phenomenon is associated with the variation in coupling between the electric field with the oxidized carbon and water molecules at lower θ, and hydroxides at higher θ. Interestingly, graphitic carbon shows a parabolic behavior with a peak at 30^{o}. This may indicate that most of the carbon atoms are situated normal to the Ru atoms where the photoionization cross-section decreases on either side of 30^{o} emission angle in the presence of varying molecular symmetry. Again, this effect is combined with the effect of photon path length through the sample at different incident angles. Therefore, we can conclude that the adsorbents are anisotropic in nature on the Ru surface, and their components may play an important role in degrading the EUV reflectivity or optical transmission[18].

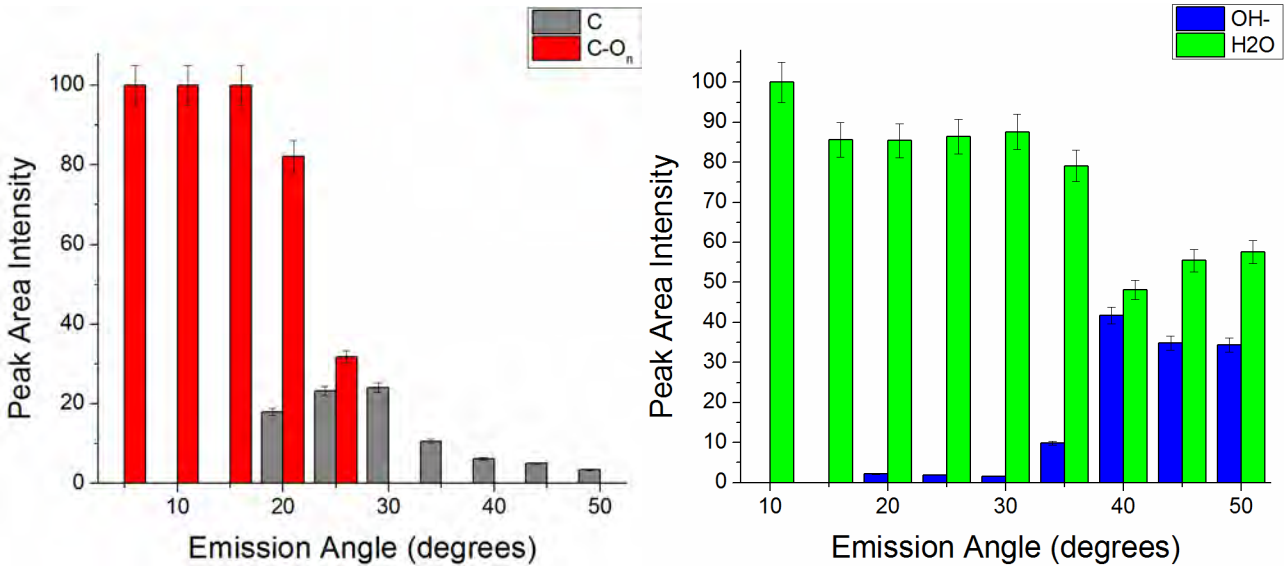

Figure 3: Components derived from Ru 3d and O 1s regions: Left part represents the relative peak area intensity of C and C-O_n from the Ru 3d, whereas right part shows the relative peak area intensity of OH and H_2O from the O1s region.

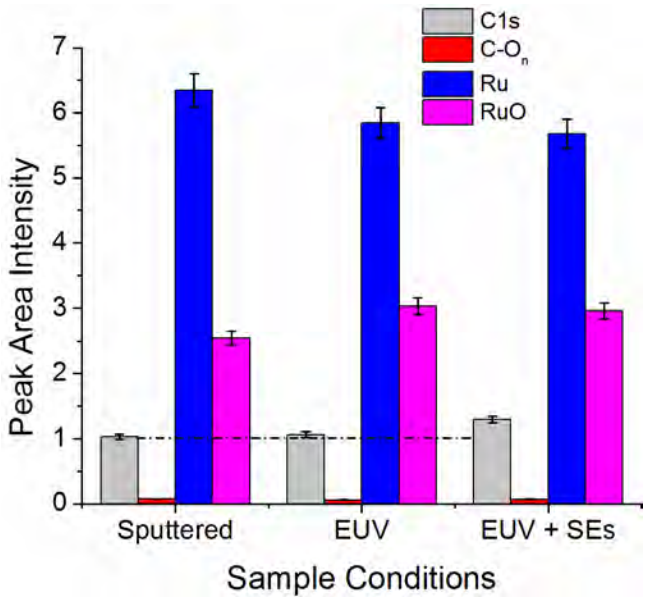

Fig 4: Effects of EUV radiation alone and in presence of the additional SEs from the focusing Ru mirror of the EUV setup on the surface components on sputter cleaned Ru films. The dotted line is a guide for the eyes.

The effects of SEs along with the 92 eV EUV beam were then examined as can be seen in Fig. 4. To screen out the electrons, a magnet was placed immeadiately after the Ru ellipsoidal mirror. The same components were measured as in the previous experiment. Detailed analysis suggests about 5% decrease in metallic Ru (Ru^0) after screening out energetic SEs during EUV exposure along with a slight increase in C concentration. By allowing additional SEs during EUV exposure, the C concentration is increased by 2%, whereas the Ru^0 is reduced by 7%. The FWHM of the RuO_2 was found to be larger than that of the respective components for Ru^0. This is most likely associated with the thickness of the oxidized Ru layers near the surface[19]. In absence of additional electrons, the low fluence of SEs from the exposed Ru surface initiates a reaction of water molecules with deposited carbon atoms (self-cleaning process)[3], while the reaction rate decelerates through surface defect mediated oxidation of the Ru surface[20] in time. These reactions could be associated with two simultaneous phenomena occurring at the Ru surface. First, the background water vapor that is dissociated by the EUV radiation can increase the free O concentration and initiate oxidation of the Ru surface. Second, the breakdown of hydrocarbons in the chamber can result in an increase in carbon atoms[6] which can react with free O atoms to form[6] CO/CO_2, and at the same time reduce the ability of the Ru substrate to adsorb/dissociate water molecules[6].

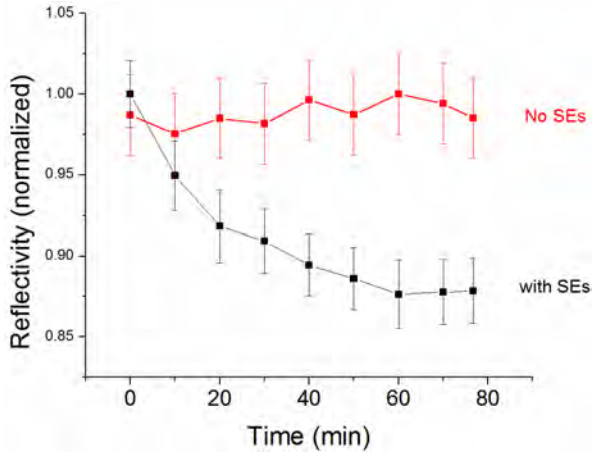

Fig 5: Reflectivity with time in the presence and absence of secondary electrons. Each data point represents one minute average.

Fig. 5 shows time dependent variation of the normalized EUVR from sputter cleaned Ru surface under discrete EUV exposure in the presence and absence of SEs. Two very different trends stand out between these data. The EUVR signal without screening SEs undergoes an exponential decay for about an hour before stabilizing. Conversely, the EUVR shows very stable signal for the duration of the test by screening additional SEs. It is important to note that the base pressure in the chamber remained similar in each experiment. It is also important to note that the EUV light itself without SEs can contaminate the surface, though it is not as severe as in case of the EUV exposed Ru layer with additional SEs. Therefore, the additional SEs in the presence of EUV light may play a dominant role in dissociating water mlecules as well as residual hydrocarbons than that of EUV light alone (see Fig. 4). Further analysis is needed to understand the full effect of this behavior.

4. CONCLUSIONS

In summary, angle-resolved XPS investigations show the anisotropic behavior of adsorbate on Ru films, where the probability of the components of the adsorbed species to interact with the incident X-rays varies with various observed emission angles θ based on their polarization directions and the path length of the incident photons. Detailed XPS analyses suggest that the water molecules and oxidized carbon are oriented towards lower observation angles θ in our setup, and thus play a key role during grazing angle reflection. Since the OH radicals are aligned towards higher θ, their existence could be critical for regulating optical transmission. We have shown that the time dependent change in carbon and oxygen on the Ru surface affects EUV reflectivity, particularly in the presence of additional electrons from the focusing Ru mirror of the EUV setup. XPS results show that the relative percentage of carbon is increased when exposed to EUV light without screening out additional electrons. The stable reflectivity by screening out excess electrons has been explained via competition between the oxidation and carbonization of the Ru mirror surface through dissociation of water molecules and hydrocarbons by EUV radiation. More work with higher accuracy is needed to fully understand the implications of these phenomena.

ACKNOWLEDGEMENTS

This work is partially supported by SEMATECH Inc. and Purdue University. The authors thank Matthew Fields for the initial experimental help.

REFERENCES

[1] Belau, L., Park, J. Y., Liang, T., Seo, H. *et al.*, "Chemical effect of dry and wet cleaning of the Ru protective layer of the extreme ultraviolet lithography reflector," Journal of Vacuum Science & Technology B, 27(4), 1919-1925 (2009).

[2] Over, H., He, Y. B., Farkas, A., Mellau, G. *et al.*, "Long-term stability of Ru-based protection layers in extreme ultraviolet lithography: A surface science approach," Journal of Vacuum Science & Technology B, 25(4), 1123-1138 (2007).

[3] Yakshinskiy, B. V., Wasielewski, R., Loginova, E., Hedhili, M. N. *et al.*, "DIET processes on ruthenium surfaces related to extreme ultraviolet lithography (EUVL)," Surf. Sci., 602(20), 3220-3224 (2008).

[4] Shin, H., Sporre, J. R., Raju, R., and Ruzic, D. N., "Reflectivity degradation of grazing-incident EUV mirrors by EUV exposure and carbon contamination," Microelectronic Engineering, 86(1), 99-105 (2009).

[5] Bajt, S., Edwards, N. V., and Madey, T. E., "Properties of ultrathin films appropriate for optics capping layers exposed to high energy photon irradiation," Surface Science Reports, 63(2), 73-99 (2008).

[6] Madey, T. E., Faradzhev, N. S., Yakshinskiy, B. V., and Edwards, N. V., "Surface phenomena related to mirror degradation in extreme ultraviolet (EUV) lithography," Appl. Surf. Sci., 253(4), 1691-1708 (2006).

[7] Hollenshead, J., and Klebanoff, L., "Modeling radiation-induced carbon contamination of extreme ultraviolet optics," Journal of Vacuum Science & Technology B, 24(1), 64-82 (2006).

[8] Kyriakou, G., Davis, D. J., Grant, R. B., Watson, D. J. *et al.*, "Electron Impact-Assisted Carbon Film Growth on Ru(0001): Implications for Next-Generation EUV Lithography," J Phys Chem C, 111, 4491-4494 (2007).

[9] Chen, J., Louis, E., Lee, C. J., Wormeester, H. *et al.*, "Detection and characterization of carbon contamination on EUV multilayer mirrors," Optics Express, 17(19), 16969-16979 (2009).

[10] Madey, T., Faradzhev, N., Yakshinskiy, B., and Edwards, N., "Surface phenomena related to mirror degradation in extreme ultraviolet (EUV) lithography," Applied Surface Science, 253(4), 1691-1708 (2006).

[11] Egbert, A., Mader, B., Tkachenko, B., Ostendorf, A. *et al.*, "Compact electron-based extreme ultraviolet source at 13.5 nm," Journal of Microlithography Microfabrication and Microsystems, 2(2), 136-139 (2003).
[12] Egbert, A., Tkachenko, B., Becker, S., and Chichkov, B. N., "Compact electron-based EUV source for at-wavelength metrology," SPIE Proceedings, 5448, 693-703 (2004).
[13] Marbach, J., Bronold, F. X., and Fehske, H., "Auger de-excitation of metastable molecules at metallic surfaces," Phys Rev B, 84(8), (2011).
[14] Ghosh, P. K., [Introduction to Photoelectron Spectroscopy] Wiley, USA, 278-282 (1983).
[15] Vinodh, M. S., and Jeurgens, L. P. H., "Quantitative analysis of angle-resolved XPS spectra recorded in parallel data acquisition mode," Surface and Interface Analysis, 36(13), 1629-1636 (2004).
[16] Mun, C., Ehrhardt, J., Lambert, J., and Madic, C., "XPS investigations of ruthenium deposited onto representative inner surfaces of nuclear reactor containment buildings," Applied Surface Science, 253(18), 7613-7621 (2007).
[17] Lee, W. H., Kim, S. J., Lee, W. J., Lee, J. G. *et al.*, "X-ray photoelectron spectroscopic studies of surface modified single-walled carbon nanotube material," Appl. Surf. Sci., 181(1-2), 121-127 (2001).
[18] Catalfano, M., Kanjilal, A., Al-Ajlony, A., Harilal, S. S. *et al.*, "Adsorption dynamics and angular dependency of contaminants on Ru mirror surfaces," Journal of Applied Physics, 111, 016103 (2012).
[19] Ernst, M. A., and Sloof, W. G., "Unraveling the oxidation of Ru using XPS," Surface and Interface Analysis, 40(3-4), 334-337 (2008).
[20] Blume, R., Niehus, H., Conrad, H., and Böttcher, A., "Surface-Defect-Mediated Channel for Oxygen Incorporation into Ru(0001)," The Journal of Physical Chemistry B, 108(38), 14332-14339 (2004).